JOURNAL OF CATALYSIS 72, 347–363 (1981)

The Hydrogenation of Carbon Monoxide over Rhodium Oxide Surfaces

P. R. WATSON AND G. A. SOMORJAI

Materials and Molecular Research Division, Lawrence Berkeley Laboratory, and Department of Chemistry, University of California, Berkeley, California 94720

Received June 24, 1981; revised August 19, 1981

Hydrated and anhydrous rhodium oxides, $Rh_2O_3 \cdot 5H_2O$ and Rh_2O_3 crystallites, were used as catalysts for the hydrogenation of CO at 6 atm and in the range of 250–350°C. The anhydrous oxide reduced to metallic rhodium rapidly, while the hydrated oxide was quite stable under the reaction conditions. The hydrated oxide produces a high concentration of oxygenated hydrocarbons, mostly acetaldehyde in addition to C_2–C_5 alkenes and methane, in contrast to the unsupported metal which is a mediocre methanation catalyst. The activation energy for the formation of all of the products is 26 ± 2 kcal/mole indicating that they are likely to be produced from a common precursor intermediate, C_xH_y. The addition of ethylene to CO and H_2 results in the conversion of the olefin to propionaldehyde. This carbonylation reaction was not observed on the rhodium metal. The slower rates of hydrogenation on the oxide and its ability to insert CO into the C_xH_y intermediates appear to be responsible for the changed product distribution in the CO/H_2 reaction. Electron spectroscopy studies indicate the presence of patches of oxide and metal both participate in the reaction and control the product distribution.

1. INTRODUCTION

The catalysis of the hydrogenation of carbon monoxide over the Group VIII metals can lead to a variety of products, the rate of formation of which depends upon the catalyst and the reaction conditions. The product spectrum can contain alkanes, alkenes, and oxygenated hydrocarbons, alcohols, and aldehydes. Rhodium catalysts of various formulations have been explored for use in both heterogenous (*1–3*) and homogenous (*4*) processes. An attractive feature of many of these catalysts is their ability to produce large yields of oxygenated products selectively, often containing two carbon atoms. Using heterogeneous rhodium catalysts, the relative amount of oxygenated products depends both on the support used and the method of deposition of the rhodium on the support. High yields of methanol and ethanol for Rh on MgO or ZnO (*2*), acetaldehyde and acetic acid for Rh on silica (*3, 28*) have been reported which contrast with results reported for alumina-supported rhodium (*1*) and rhodium foil (*5*) in which only hydrocarbon products that contained no oxygen were detected.

In this laboratory we have explored the characteristics of small-surface-area rhodium crystals (*5*) for the hydrogenation of CO at pressures in the range of 1–10 atm. Such systems are model catalysts free of support effects which can reveal the influence of surface structure and composition upon their activity and selectivity. These studies have shown that clean elemental rhodium is a stable methanation catalyst, but of mediocre activity. Preoxidation of the surface of a rhodium single crystal or foil results in sharply enhanced activity for methanation and the formation of small but detectable amounts of oxygenated species.

The changing product distribution and activity obtained upon preoxidation of the rhodium metal samples (*6*) have prompted us to extend such studies to the rhodium–oxygen system in general. This system is

0021-9517/81/120347-17$02.00/0

rather poorly understood as rhodium oxides appear to be thermodynamically unstable under the reaction conditions utilized during the catalyzed hydrogenation of CO. We present results obtained for CO hydrogenation over rhodium oxide surfaces obtained from both the hydrated and anhydrous sesquioxide and the dioxide. The differing stabilities of these compounds under reaction conditions have been uncovered and explored. The surface composition and oxidation state were monitored both before and after reaction by Auger electron spectroscopy (AES), X-ray photoelectron spectroscopy (XPS), and thermal desorption spectroscopy (TDS). The reaction was carried out at about 6 atm pressure using temperatures between 250 and 350°C and various H_2/CO ratios.

Our results indicate that the hydrated oxide can be kinetically stabilized for hours under the reducing conditions of the CO/H_2 reaction. The oxide produces up to 30% oxygenated products at low conversions, mostly acetaldehyde. The activation energies to produce methane, ethylene, and acetaldehyde, are all about the same, 26 ± 2 kcal/mole indicating that these molecules form from a common precursor. The addition of ethylene to the CO/H_2 feed led to its conversion to propionaldehyde. Carbonylation activity observed on the rhodium oxide was absent for rhodium metal under identical reaction conditions. The reaction mechanism that can be proposed includes the rate-determining formation of C_xH_y fragments, followed by the rapid carbonylation or hydrogenation of these intermediates to form the observed reaction products. The reduced hydrogenation and increased carbonylation activity of the rhodium oxide as compared to the metal is thought to be responsible for the markedly altered product distribution.

2. EXPERIMENTAL

The experimental apparatus, described in detail elsewhere (*5*, *7*), consists of an ultrahigh vacuum chamber pumped with ion and diffusion pumps and equipped with retarding field LEED/Auger optics, a mass spectrometer, and an internal high-pressure (<20 atm) isolation cell. With the cell open, samples can be cleaned by argon ion sputtering, annealing, or chemical treatments with gases admitted via a leak valve. Surface composition was monitored regularly by AES. With the cell closed, the apparatus was operated as a stirred batch reactor. The CO (Matheson, 99.95%) was passed through a copper tube heated to ~200°C and then through a molecular sieve chilled by an acetone–dry ice bath to remove carbonyls; the H_2 (Liquid Carbonic, 99.995%) was used without further purification. Reaction products were monitored by diverting a very small fraction of the gases to a gas chromatograph (Hewlett–Packard 5720A) equipped with a flame ionization detector and integrator (Spectra Physics). Due to the low conversion levels (<1%) such a detector is required, but unfortunately prevents a carbon and oxygen balance due to its insensitivity to permanent gases. A 6-ft × 1/8-in. Porapak PS column initially held at 50°C for 5 min and then temperature programmed at 6°/min allowed a good on-line separation of all major oxygenated and hydrocarbon products in a 15- to 20-min analysis.

XPS measurements were carried out in a separate instrument, a modified AES 200 spectrometer. This instrument did not allow for sample treatment and operated under only modest vacuum conditions of $\sim 5 \times 10^{-8}$ Torr and, hence, was only suitable for examination of metal spectra. An Al$K\alpha$ source was used, and the hemispherical analyzer was equipped with position-sensitive, pulse-counting electronics which allowed good signal-to-noise spectra to be accumulated rapidly. Binding energies were referred to C 1*s* at 285.0 eV; the resolution of the instrument was about 1.8 eV. Samples were mounted on double-sided adhesive tape.

High-pressure CO hydrogenation reactions were carried out over various rho-

dium oxide samples which were deposited as thin layers from a methanol slurry onto gold (and occasionally platinum) foils. The metal foils provided both a physical backing for these powder samples and a means of heating. The foils were heated resistively both to outgas the samples and to establish reaction temperatures, which were measured by an Alumel–Chromel thermocouple attached to the foil.

The rhodium oxide samples used were (a) anhydrous RhO_2 (Alfa Products), (b) anhydrous Rh_2O_3 (Aldrich Chemical Co.), and (c) $Rh_2O_3 \cdot 5H_2O$ (Pfaltz and Bauer, 99.9%). The anhydrous oxides were used as purchased. After deposition as a film, and mounting in the vacuum chamber on Au or Pt foils, they were degassed at 400°C for 1 h and then surface impurities were removed by ion bombardment. The hydrated sesquioxide was heated in air at ~400°C prior to deposition on the Au foil. The exact temperature at which this heating was carried out did not appear to be important as regards the catalytic properties of the resulting oxide. Thermogravimetric analysis of the dehydration of the $Rh_2O_3 \cdot 5H_2O$, however, showed that the dehydration reaction is complex and gradual.

The surface area of the dried sesquioxide before deposition was estimated by the BET method and found to be ~10 m^2/g.

3. RESULTS

3.1. Surface Characterization

a. Anhydrous Rh_2O_3 and RhO_2 AES Measurements

The Auger spectra obtained using the RFA analyzer were, in general, free of charging effects, probably due to the thin oxide layers and the proximity of the high-

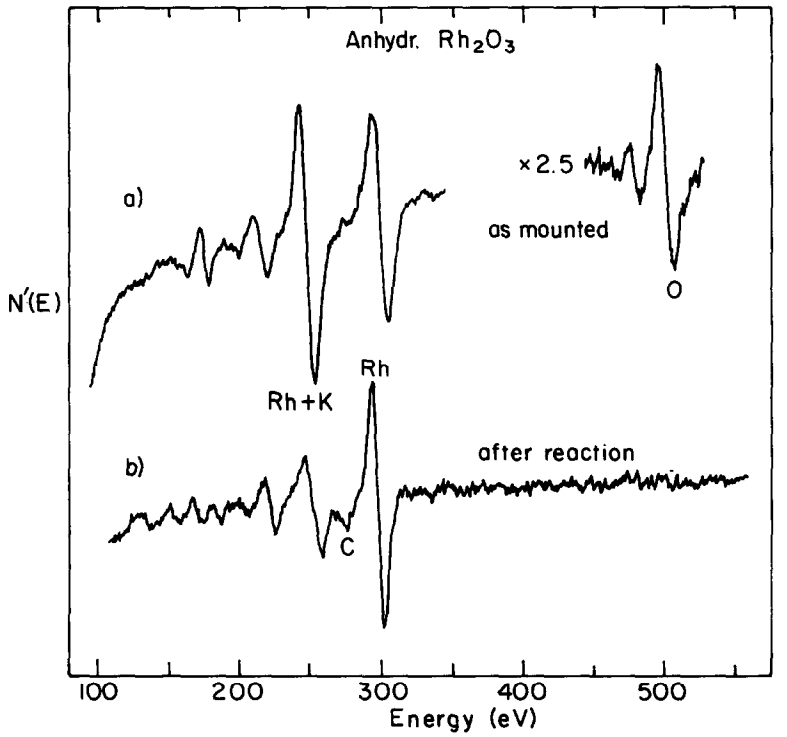

FIG. 1. Auger electron spectra of an anhydrous Rh_2O_3 surface: (a) as mounted in the vacuum chamber; (b) after reaction at 300°C, 6 atm in 1 : 1 H_2/CO.

conductivity metal support. In some cases, particularly after a reaction, rather noisy spectra result, e.g., Fig. 3c, but generally quite clean spectra could be obtained, e.g., Fig. 1.

The anhydrous sesquioxide, Rh_2O_3, exhibited an Auger spectrum after mounting in the vacuum chamber, as shown in Fig. 1a. The oxygen transition at 515 eV is pronounced, being about one-fourth of the intensity of the main rhodium transition at 302 eV. The large peak at ~225 eV is composite, being made up of a rhodium transition at 256 eV and an overlapping potassium transition at 252 eV. Due to the strong cross section of potassium and the low resolution of the RFA analyzer, a relatively small contamination of potassium results in a 255-eV peak larger than that for pure rhodium where $I^{255}/I^{302} \sim 0.3$–0.4

After reaction in 6 atm of 1 : 1 H_2/CO at 300°C for 30 min, the Auger spectrum of Fig. 1b is obtained. Clearly, the potassium peak has diminished but, most importantly, the oxygen peak is now entirely absent, indicating reduction to the metal. This reduction can be followed visually by a color change from the black oxide to the silver–gray metal.

Figure 2 shows a sequence of Auger spectra for the anhydrous dioxide, RhO_2. The freshly mounted specimen showed an O^{515}/Rh^{302} ratio of 0.32 and the presence of potassium on the surface. Degassing at 400°C for 1 h changed the color of the sample from brown to black; the surface concentration of potassium dropped, presumably due to desorption or migration into the bulk; the O^{515}/Rh^{302} ratio dropped to about 0.2 close to the value obtained for Rh_2O_3. This indicates a decomposition of the dioxide to the sesquioxide, a reaction known to

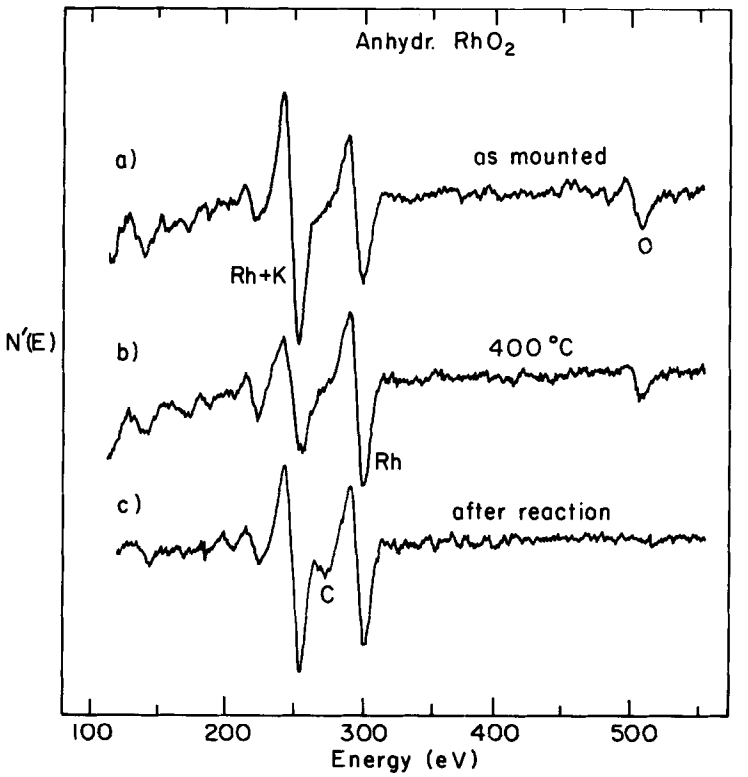

FIG. 2. Auger electron spectrum of an anhydrous RhO_2 surface: (a) as mounted in the vacuum chamber; (b) after heating to 400°C for 1 h; (c) after reaction at 300°C, 6 atm in 1 : 1 H_2/CO.

occur at about 680°C at 1 atm (*30*):

$$2RhO_2 \rightarrow Rh_2O_3 + \tfrac{1}{2}O_2.$$

Once again reaction of 1 : 1 H_2/CO at 6 atm, 300°C resulted in complete reduction to the metal as evidenced by Fig. 2c, together with the reemergence of some potassium and some deposition of carbon.

b. Hydrated Rhodium Sesquioxide $Rh_2O_3 \cdot 5H_2O$—AES, XPS, and TDS Measurements

The hydrated sesquioxide behavior was markedly different from its anhydrous counterpart. In order to avoid excessive outgassing in the vacuum chamber, the oxide was first heated in air to 400°C or more for 2 h. Dehydration appears to be a complex and kinetically slow process and results in an oxide with considerably more stability and resistance against reduction to the metal than the anhydrous oxide. This is evidenced in the Auger spectra shown in Fig. 3. The first spectrum shows an asmounted spectrum of the hydrated sesquioxide which appears similar to that of the anhydrous oxide. Figure 3b shows a spectrum of the oxide after degassing and cleaning by ion bombardment in the vacuum chamber and shows a lowered potassium level and only a small reduction in the surface oxygen concentration. However, reaction in H_2/CO under the same conditions that reduced the anhydrous sesqui- and dioxides to the metal does not reduce

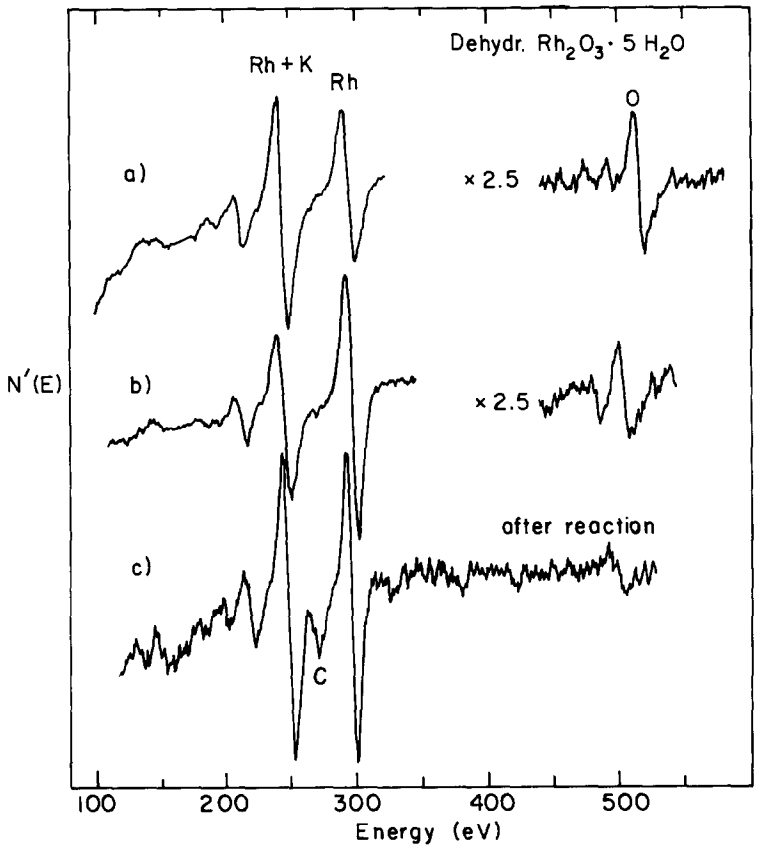

FIG. 3. Auger electron spectrum of a $Rh_2O_3 \cdot 5H_2O$ sample dried at 600°C for 2 h: (a) as mounted in the vacuum chamber; (b) after heating to 400°C for 1 h and then argon ion bombarded at 500 eV and 5 $\mu A/cm^2$ for 15 min; (c) after reaction at 300°C, 6 atm in 1 : 1 H_2/CO.

the dehydrated oxide totally, but leaves a small but readily detectable oxygen concentration (Fig. 3c), and also does not induce the black–gray color change. This oxygen surface concentration gives rise to the Auger peak ratio, $O^{515}/Rh^{302} \sim 0.1$–$0.2$. Thus the CO/H_2 reaction over the hydrated sesquioxide produces an oxygen-deficient surface region which is, however, relatively stable to reduction under hydrogenation reaction conditions. The stable oxide formed in this manner can be reduced to the metal by (1) heating to >400°C *in vacuo* with carbon present, e.g., after a synthesis reaction, leading to production of CO_2 and reduction,

$$2C_{lattice} + Rh_2O_3 \rightarrow CO + CO_2 + 2Rh,$$

(2) heating to >400°C in excess H_2, (3) heating *in vacuo* to >550°C, or (4) many hours of reaction in H_2/CO mixtures will eventually lead to reduction.

XPS spectra were recorded in a separate apparatus for the Rh $3d_{5/2}$ line. Due to the modest vacuum of this spectrometer and the fact that the samples had to be transferred in air and could not be treated *in situ*, no analysis of C 1*s* or O 1*s* signals was attempted. Table 1 shows XPS data for rhodium metal and the used catalyst, together with $Rh_2O_3 \cdot 5H_2O$, $Rh_2O_3 \cdot 5H_2O$ dried at 400°C for 2 h, and anhydrous Rh_2O_3. A progressive shift of the position of the rhodium $3d_{5/2}$ peak from a value of 308.5 eV for the metal through to 311.0 eV for Rh_2O_3 is found. The peak maxima found in our studies are also compared with values given by Brinen and Malera (*10*). The shift in binding energy between Rh and Rh_2O_3 is the same for the two sets of results within 0.1 eV, but the absolute values differ by about 1.5 eV, a discrepancy which may be due to charging effects. We also note that our values for the Rh(III) compounds are quite close to that given by Jørgensen and Berthou (*11*) for $RhCl_3$ of 310.5 eV.

TABLE 1

XPS Binding Energy Data for the Rh $3d_{5/2}$ Line

Sample	E_B Rh $3d_{5/2}$		
	This work	ΔE_B	Brinen and Malera (*10*)
Rh metal	308.5 ± 0.2	2.8	307.1
$Rh_2O_3 \cdot 5H_2O$	311.0 ± 0.2	2.2	
Dried $Rh_2O_3 \cdot 5H_2O$	309.8 ± 0.2	1.9	
Anhydrous Rh_2O_3	310.0 ± 0.2	2.5	308.7
Used catalyst	309.0 ± 0.2	2.4	

Note. Binding energies are referred to C 1*s* at 285.0 eV. ΔE_B represents the full width at half-height of the Rh $3d_{5/2}$ peak.

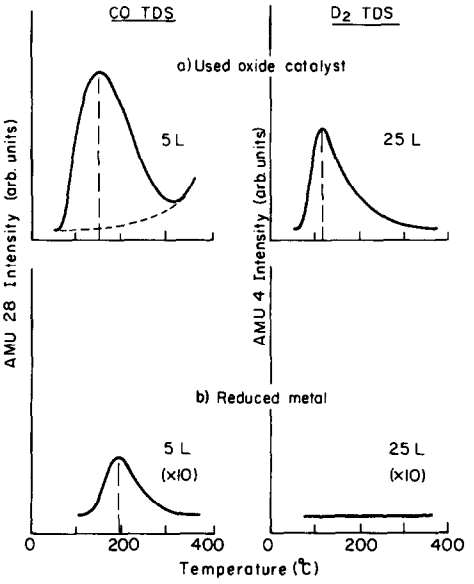

FIG. 4. Thermal desorption spectra of CO and D_2 from: (a) a used oxide catalyst; (b) the same catalyst reduced to the metal by heating *in vacuo* to 750°C for 30 min and subsequently cleaned by ion bombardment.

These data clearly indicate that the starting material used in the majority of these experiments, $Rh_2O_3 \cdot 5H_2O$ that had been heated for 2 h or more at 400°C, contains rhodium in a high oxidation state close to a formal charge of 3. The used catalyst, however, displays a Rh $3d_{5/2}$ binding energy value that is much closer to that of metallic rhodium but still indicates the presence of rhodium in a partially oxidized form.

While the resolution of our XPS instrument is modest, the peak width (at half-height) data shown in Table 1 show that heating the hydrated sesquioxide results in a rather sharp peak indicating that all the rhodium present is in a similar chemical environment. The anhydrous oxide, the metal, and the used catalyst, however, show rather wide peaks that indicate the presence of other surface oxide phases or a mixture of oxide and rhodium metal environments (*8, 9*).

Thermal desorption of both CO and D_2 was also performed. On the freshly prepared hydrated oxide surface only small amounts of CO and D_2 (<15 and <5%, respectively) were detected desorbing. The vast majority of the reactant gases were desorbed as either CO_2 or D_2O, indicating facile reduction of lattice oxygen. Further details of this work will be published elsewhere.

On an oxide surface that has been used as a catalyst, both CO and D_2 desorb as intact molecules. Typical desorption spectra are shown in Fig. 4a; while CO adsorption continued almost indefinitely (up to several thousands of Langmuires exposure) the D_2 desorption peak is saturated at exposures of ~250 L.

This behavior with D_2 may be attributable to the rapid conversion of the remaining oxide sites on the surface to hydroxyl. D_2 can then only be desorbed by the breaking of these O–H bonds and subsequent migration and recombination of D atoms resulting in a relatively high temperature of desorption.

In Fig. 4b, the above results are compared with TDS results for CO and D_2 adsorbed onto a catalyst that had been reduced by high-temperature decomposition of the oxide to the metal. Two effects of reduction are immediately apparent. First, D_2 desorbs from the reduced metal surface close to room temperature, in agreement with other studies of the H_2/Rh system (*5, 31, 32*); whereas it desorbs at the relatively high temperature of ~120°C from the oxide surface. Reduction of the oxide appears to lower the amount of CO adsorbed, but also increases the binding energy of that CO, evidenced by the upward shift of the peak maximum from ~150 to 190°C, a value somewhat lower but close to the range normally found for CO desorption from metallic rhodium (*32*).

3.2. Reaction of H_2/CO over Rhodium Oxides

a. Background Reactivity

In order to assess the background reactivity of the system and of the metallic foils used as backings for the oxide films, blank experiments were performed with Au and Pt foils. The results of these tests are presented in Table 2 and are compared with results for deposited films of hydrated $Rh_2O_3 \cdot 5H_2O$ on gold foil (for more detail see Section 3.2c). As a comparative measure of the rates of reaction, the number of C atoms converted to products during 1 h is listed for typical samples. Also listed are the product distributions.

Clearly, the metal foils in the stainless-

TABLE 2

Reaction of 1 : 1 H_2/CO at 6 atm Pressure over Au and Pt Foils Compared with Dried $Rh_2O_3 \cdot 5H_2O$ on Au Foil

Sample	T (°C)	Total C atoms converted in 60 min	Product distribution (wt%)				
			C_1	C_2	C_3	C_{4+}	Oxys
Au foil	300	6×10^{16}	64	19	13	4	0
Pt foil	350	25×10^{16}	87	7	2	3	0
Dried rhodium oxide on Au foil	350	190×10^{16}	41	17	13	5	23

steel reaction chamber give a very different product distribution containing no oxygenates when compared to a rhodium oxide film deposited on a foil. The rate of conversion to products in the presence of the blank foils is an order of magnitude less than when the foils are covered with rhodium oxide. Samples of oxide deposited on either type of Pt or Au foil behave in a very similar manner. Therefore, as the foil supports are completely covered during the experiments with a rhodium oxide film, we can be certain that any oxygenated products we see are due to the presence of the rhodium oxide.

b. Reaction over Anhydrous RhO_2 and Rh_2O_3

Both of these anhydrous oxides were rapidly and completely reduced to the metal in a H_2/CO mixture. The reduction was evidenced by (1) an obvious color change from the characteristic oxide color of brown (RhO_2) or black (Rh_2O_3) to a silvery-gray metallic luster characteristic of rhodium metal; (2) the disappearance of an oxygen Auger signal is noted in Section 3.1 and shown in Figs. 1 and 2; (3) a product distribution typical of rhodium metal showing little or no oxygenates present and a predominance of methane (80%+).

Attempts were made to reoxidize reduced samples of these materials by heating in wet and in dry O_2 at 1 atm pressure and at 600°C for 30 min. After such treatments the oxide formed was still found to be unstable and reduced to the metal very rapidly under reaction conditions in the $CO-H_2$ gas mixtures. Due to the extreme instability of these oxides no further studies were made of their catalytic properties.

c. Reaction over Hydrated $Rh_2O_3 \cdot 5H_2O$

1. Product distributions. As mentioned in Section 3.1, the hydrated sesquioxide is relatively stable under reaction conditions and can be operated for many hours in a mixture of H_2 and CO with only slow reduction occurring.

The hydrogenation of CO over a hydrated $Rh_2O_3 \cdot 5H_2O$ surface leads to the formation of large concentrations of oxygenated hydrocarbons. A yield of oxygenated products can be detected that may be

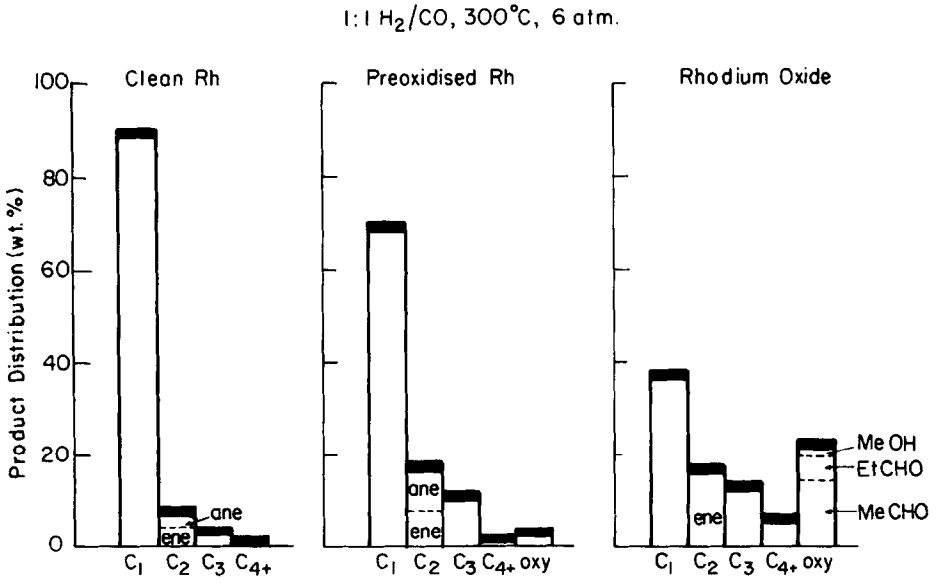

FIG. 5. Product distribution (wt%) for the reaction of 1:1 H_2/CO at 300°C and 6 atm pressure for rhodium oxide ($Rh_2O_3 \cdot 5H_2O$) compared with rhodium metal both clean and preoxidised (6).

TABLE 3

Product Distributions for CO Hydrogenation over Various Rhodium Catalysts

Catalyst	T (°C)	P (atm)	H_2/CO	Product distribution (C at.%)							Ref.
				C_1	C_2	C_3	MeOH	EtOH	MeCHO	MeCOOH	
Rh/Al_2O_3	265	1	3	89	8	3	0	0	0	0	(*1*)
Rh metal	300	6	3	91	7	2	0	0	0	0	(*5*)
Rh/La_2O_3	225	0.1	2	23	1	$\ll 1$	30	46	Trace	0	(*2*)
Rh/ZnO	250	0.1	2	18	0	0	82	0	0	0	(*2*)
Rh/SiO_2	300	70	1	53	1	0	0	Trace	30	6	(*3*)
Rh/SiO_2	300	80	1	9	[a]	[a]	[a]	4	42	37	(*28*)[b]
Preox. Rh	300	6	3	80	11	7	Trace	Trace	2	0	6
Dried $Rh_2O_3 \cdot 5H_2O$	300	6	3	29	22	25	3	Trace	16	0	This work

[a] Not quoted.
[b] mole%.

as high as 25 wt% or more, depending upon the reaction conditions. This sequence is shown in more detail in Fig. 5 where the product distributions obtained for $Rh_2O_3 \cdot 5H_2O$, rhodium metal, and the oxidized metal are reported.

Acetaldehyde is the major oxygen-containing product together with smaller amounts of propionaldehyde, butyraldehyde, methanol, and trace amounts of ethanol. Acetic acid and its esters were not detected, although the analytical method used was capable of detecting such products. An interesting feature is that the C_{2+} hydrocarbon yield is almost entirely olefinic, in contrast to the usual predominance of alkanes with the metallic rhodium catalysts.

Table 3 compares the product distribution from this $Rh_2O_3 \cdot 5H_2O$ catalyst with other literature reports for rhodium catalysts. The results for this rhodium catalyst approach those reported by Wilson and coworkers (*3*) for a silica-supported catalyst operated at somewhat higher pressures and higher conversion than those used here. The silica-supported catalyst produces large amounts of acetic acid and ethanol, while the dehydrated rhodium oxide used here produces predominantly acetaldehyde. It is possible that at high conversion or pressures acetaldehyde may be formed initially and then further reacted to form these other products.

It is intriguing to speculate on the differences in behavior among these various rhodium catalysts and as to their origin. Our results suggest that the degree of oxidation of the rhodium may be an important factor, metallic rhodium formulations (*1*, *5*) leading to hydrocarbons and oxidized forms leading to more oxygenated products

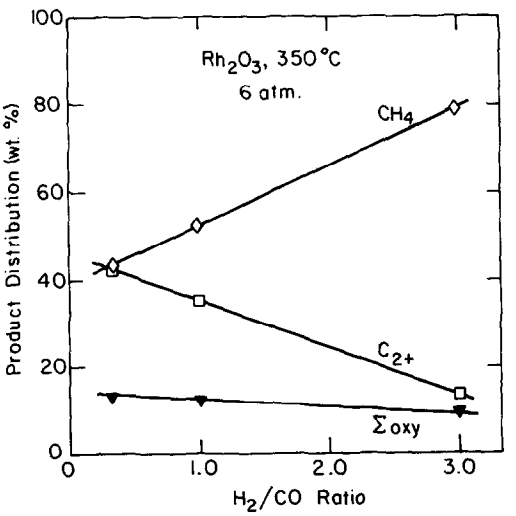

FIG. 6. The effect of changing the H_2/CO ratio on the product distribution of the hydrogenation of CO over dried $Rh_2O_3 \cdot 5H_2O$ at 350°C and 6 atm.

(*2, 3, 6, 28*). Clearly, the method of preparation and pretreatment of these catalysts is all important and should be characterized more fully.

The effect of changing the H_2/CO ratio is shown in Fig. 6 for a sample held at 6 atm total pressure and 350°C. The percentage of oxygenated products is relatively insensitive to this parameter, although a slight trend to more alcoholic products is seen at higher H_2 partial pressures as might be expected. The major effect of increasing the CO concentration in the reactant stream is to depress the methane yield and increase the amount of C_2–C_4 hydrocarbons formed such that they are formed in roughly equal (wt%) amounts for a 1 : 3 H_2/CO mixture.

As is demonstrated in Fig. 7, the effect of changing the total pressure over the range of 2–10 atm at fixed temperature and synthesis gas composition is very small.

The effect of increasing the reaction temperature upon the product distribution is shown in Fig. 8. Raising the temperature favors the production of shorter-chain hydrocarbons presumably by preferentially increasing the rate of hydrogenation relative to that of chain growth. Conversely, lowering the temperature increases the total yield of oxygenated products; unfortunately, at temperatures of 250°C and below the rate of conversion is sufficiently low to make accurate determination of the oxygenate yields difficult.

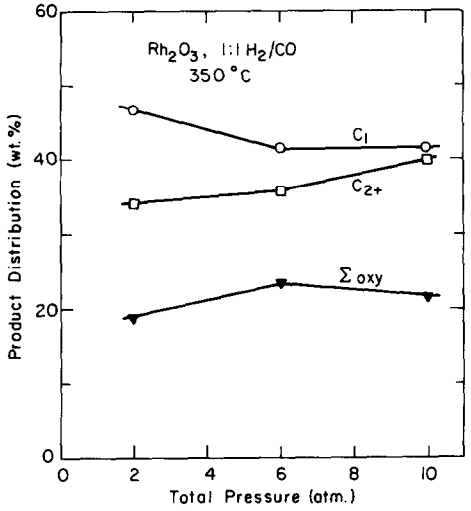

FIG. 7. The effect of changing the total pressure on the product distribution for the reaction of 1 : 1 H_2/CO at 350°C over dried $Rh_2O_3 \cdot 5H_2O$.

2. Kinetics. A typical plot of the accumulation of products with time is shown in Fig. 9 for a gold-supported, hydrated $Rh_2O_3 \cdot 5H_2O$ film at 300°C, 6 atm pressure, and

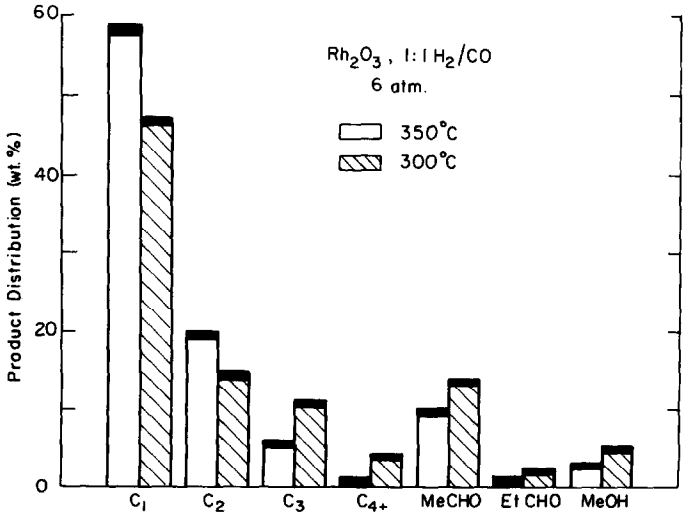

FIG. 8. The product distribution in weight percent at temperatures of 350 and 300°C for the reaction of 1 : 1 H_2/CO at 6 atm over dried $Rh_2O_3 \cdot 5H_2O$.

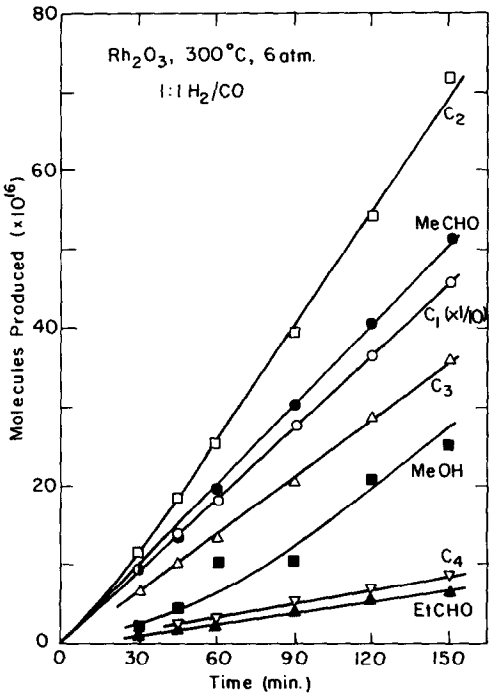

FIG. 9. Product accumulation with time for the reaction of 1 : 1 H_2/CO at 300°C and 6 atm over dried $Rh_2O_3 \cdot 5H_2O$.

1 : 1 H_2/CO ratio. We can see that all products are produced at approximately constant rates with little or no induction period and with no drop in performance over a period of 2–3 h. Occasionally poisoning by sulfur led to reductions in the rates. Assigning turnover numbers (TNs) to each product is complicated by imprecise knowledge of the number of Rh atoms available for reaction; but, using the BET surface area of 10 m^2/g and assuming that two-fifths of the surface atoms are rhodium, we arrive at TNs for the major products of (1 : 1 H_2/CO, 300°C, 6 atm; $Rh_2O_3 \cdot 5H_2O$):

	CH_4	CH_3CHO
TN (molecules/site/sec)	$\sim 1 \times 10^{-3}$	$\sim 1 \times 10^{-4}$

The Ch_4 TN estimate is lower than those reported for Rh foils at 6 atm (*6*), but are closer to those reported for supported rhodium catalysts (*1*, *3*), as shown in Table 4. This discrepancy, however, may be more apparent than real as no *in situ* measure of the number of surface Rh atoms was available and, hence, the number of atoms taking part in reaction is probably overestimated. Table 4 also lists the activation energy for methane production obtained from an Arrhenius plot. The value of 26 kcal/mole, found for the dehydrated rhodium oxide used in the present work, compares very favorably with other values found for rhodium synthesis gas catalysts.

In Fig. 10 is shown an Arrhenius plot for the formation of C_1–C_3 hydrocarbons and acetaldehyde, the major oxygenated product. Within experimental error, all the

TABLE 4

Turnover Numbers for Methane Production over Dried $Rh_2O_3 \cdot 5H_2O$ Compared with Literature Data at 300°C, 1 : 1 H_2O

	CH_4 TN (molecule/site/sec)	E_A (kcal/mole)	Ref.
Rh foil, 1–6 atm, clean	0.1	24 ± 2	(*5*, *6*)
Rh/Al_2O_3, 1 atm	0.034	24 ± 2	(*1*)
Rh/SiO_2, 7 atm	0.030	24 ± 2	(*3*)
Dried $Rh_2O_3 \cdot 5H_2O$, 6 atm	0.001	26 ± 2	This work

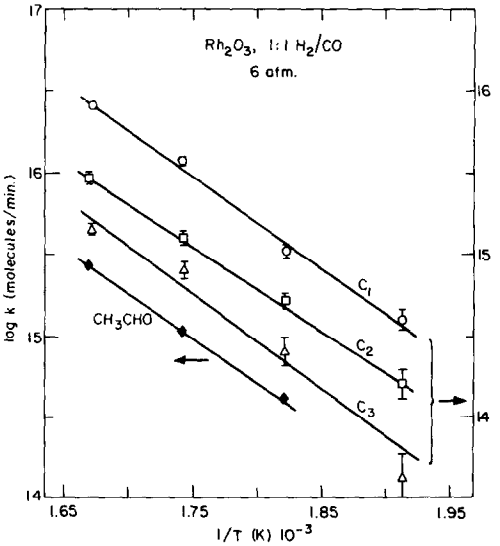

FIG. 10. Arrhenius plot of kinetic data for the reaction of 1 : 1 H_2/CO at 6 atm over dried $Rh_2O_3 \cdot 5H_2O$.

hydrocarbon species methane, ethylene, and propylene/propane, *and* acetaldehyde show variations of reaction rate with temperature that are all closely similar, and the activation energies of their formation all cluster around a value of 26 ± 2 kcal/mole.

3. Hydrogenation of carbonaceous residues. At the end of a reaction, AES and XPS reveal the presence of considerable amounts of carbon on the surface of the sample (Fig. 3c). Carbonaceous deposits formed during CO/H_2 reactions have been reported for Ni (*12–14*), Fe (*15–17*), and Rh catalysts (*5*, *6*). In common with these systems, the carbon deposits that are found on the rhodium oxide surfaces investigated can be easily hydrogenated. The results of such a hydrogenation experiment are depicted in Fig. 11. The products are solely alkanes with methane the majority product (95 wt%), although products up to C_5 can be detected. In particular, *no* oxygenated products of any type can be detected during such an experiment, even as a transitory feature.

These results are similar to those reported by Bonzel and co-workers (*16*, *17*) for the hydrogenation of carbidic residues on Fe foils, but do differ in certain respects. Under the conditions employed by these workers, the Fe foil acted as a methanation catalyst. The Fe foil produced CH_4 at the same rate from a mixture of CO and H_2 as when carbidic residues were hydrogenated.

Our experiments with rhodium oxide show a somewhat different behavior in that

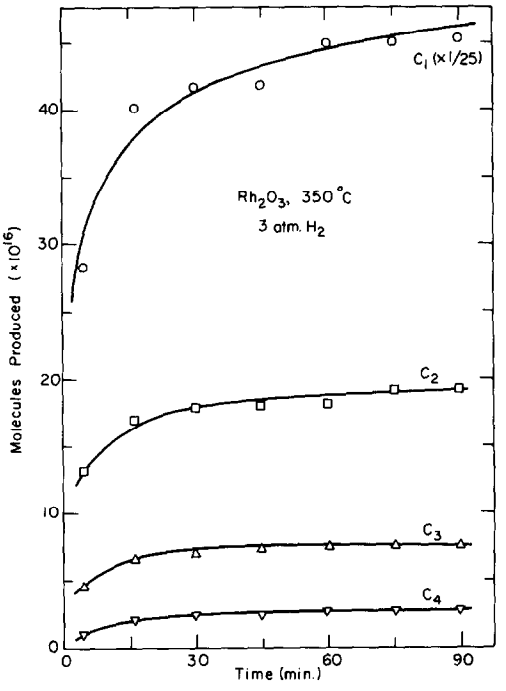

FIG. 11. Product accumulation with time for the hydrogenation of carbonaceous residue from a previous hydrogenation of CO reaction using 3 atm H_2 at 350°C.

CH_4 was produced by hydrogenation of carbonaceous deposits at initial rates of about 10–30 times the rate of methane production from CO/H_2 mixtures. As reported in Table 5, while the rate of methane production is greater under hydrogenation conditions, the initial rates of production of higher hydrocarbons (not reported by Bonzel and co-workers) are *lowered* from their CO/H_2 reaction values. Clearly, in contrast

TABLE 5

Comparison of Rates of Formation of Products Formed over Dried $Rh_2O_3 \cdot 5H_2O$ at 350°C

	P (atm)		Rate × 10^{16} molecule/min				
	CO	H_2	C_1	C_2	C_3	C_4	CH_3CHO
Reaction[a]	3	3	18.0	8.4	4.5	1.4	3.5
Hydrogenation[b]	0	3	140.0	2.6	0.9	0.45	0

[a] 1:1 H_2/CO mixture.

[b] Hydrogenation of the residue from *a*.

to the results on simple methanation catalysts, the fate of carbon deposits under reaction conditions is not the same as that under pure hydrogenation conditions. The implications for the reaction mechanism are discussed in Section 4.2.

4. The effect of added ethylene. The effect of adding a small amount of ethylene (0.1%) to the reactant gas stream is demonstrated in Fig. 12. With no added ethylene, we obtain a typical product spectrum, shown in Fig. 12a. Note that these data are product distributions for all products excluding C_2. When 0.1% C_2H_4 is present, it completely dominates the analysis and is, hence, removed from these data to more clearly show the effect on the production of other substances. In Fig. 12b are the results when 0.1% C_2H_4 is present, and we can clearly see that added ethylene is converted almost completely to propionaldehyde. This is in complete contrast to the behavior of rhodium metal where only a small increase in the concentration of higher hydrocarbons was observed (*6*).

It appears that C_2 units are being formed intact on the active surface from ethylene and then converted to C_2H_5CHO by direct

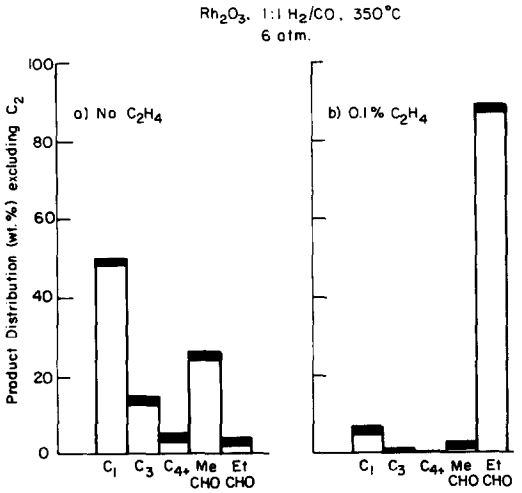

FIG. 12. Product distributions in weight percent (excluding C_2 hydrocarbons) found for the reaction of 1 : 1 H_2/CO at 6 atm and 350°C with: (a) no added C_2H_4; (b) 0.1% C_2H_4 added to the reactants.

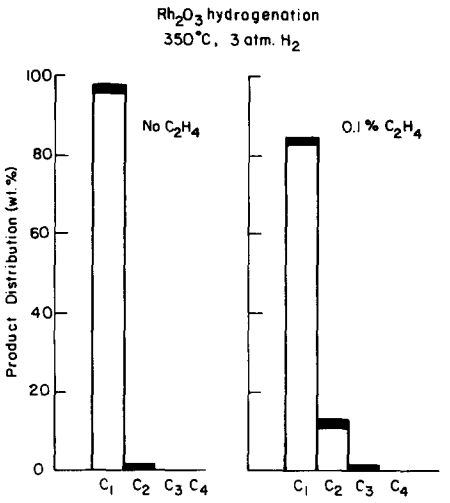

FIG. 13. Product distribution obtained from the hydrogenation of the carbonaceous residue formed in the reactions of Fig. 12 with 3 atm of H_2 at 350°C.

carbonylation. We would expect that hydrogenation of the carbon deposit from such a mixture would lead to abnormally high C_2 and C_3 hydrocarbon fractions. This is indeed the case as is shown in Fig. 13, where the product distributions for hydrogenation from carbon layers formed from CO/H_2 and $CO/H_2/0.1\%$ C_2H_4 are compared. In the presence of the ethylene additive, the C_1 fraction is markedly reduced, the C_2 fraction greatly increased, and the C_3 fraction is now measurable, clearly indicating a large fraction of C_2 species on the surface.

4. DISCUSSION

4.1. Identity and Stability of Rhodium Oxide Catalysts

The thermodynamic parameters (free energy and heat of formation) that characterize rhodium oxides (*30*) indicate that they should be unstable under the reaction conditions used during the hydrogenation of CO (>300°C, absence of oxygen). The dissociation oxygen pressure of the oxide is greater than 10^{-6} Torr at 400°C which assures its decomposition in the reducing $CO-H_2$ gas mixture. The ordered oxide

forms readily upon heating the metal in a low partial pressure of oxygen at high temperatures (*29*) followed by rapid cooling that prevents the out-diffusion of oxygen from the bulk of the metal. The trapped oxygen readily orders, and the oxide structures that form in the near-surface region have been studied by Castner and Somorjai (*29*). The rapid reduction of anhydrous rhodium oxides in CO/H_2 gas mixtures upon heating to 300°C is clearly demonstrated in this study and by previous studies of the preoxidized metal. However, we find that the hydrated rhodium oxide, $Rh_2O_3 \cdot 5H_2O$ retains a relatively high concentration of oxygen at the surface even after hours of chemical reaction in high pressures of CO and H_2 at 300°C. Thus while the metal oxide is thermodynamically unstable, it is kinetically stabilized by the slow rate of reduction of this particular form of hydrated oxides.

It is desirable to improve the characterization of the different oxides used in this study in order to understand more fully their differing stabilities. Work is under way to determine the effects of heat and reducing gases on the mode of decomposition and the modifying effect of impurities, particularly in the form of alkali metals which were present in some of our samples.

It occurs frequently in heterogeneous catalysis that a certain form of catalyst that is thermodynamically unstable remains stable indefinitely in the circumstances of chemical reaction. Zeolites (alumina silicates) of all types are metastable with respect to crystalline alumina and silica, yet they remain structurally stable to over 1000°C. Noble metal oxides, oxides of platinum, gold, and iridium, in addition to rhodium are all thermodynamically unstable, yet they are prepared and utilized as stable catalysts in proper circumstances. Their stability is assured by their slow rate of decomposition that is controlled by the diffusion of oxygen from the bulk to the surface of the metal, a very slow process indeed below 500–600°C, that is, under the usual conditions of most heterogeneous catalytic reactions.

4.2. Reaction Mechanism

The major difference between hydrated Rh_2O_3 and metallic rhodium for the hydrogenation of CO is that the oxide produces large quantities of aldehydes and the hydrocarbon product is predominantly olefinic. This clearly implies that placing rhodium atoms in an oxide environment leads to a diminution of their hydrogenation ability. Thus while rhodium metal catalyzes the formation of only small quantities of olefins compared to alkanes, the oxide catalyst produces mostly olefins. The diminished hydrogenation capability also leads to the formation of aldehydes rather than alcoholic oxygenates particularly at H_2/CO ratios of 1 or less. The different product distributions obtained during the CO/H_2 reaction over rhodium catalysts dispersed on a variety of supports (*1, 3, 28*) may well be the result of the unique oxidation rates that are stabilized by metal–support interactions.

The first question we might address is that of the source of the oxygen atoms that appear in the oxygenated products—do they arise from CO or from the lattice oxygen? In the absence of isotopic labeling evidence, which is not practical in this experimental arrangement, we must turn to indirect evidence. There is, in fact, good indirect evidence that in the main the oxygen atoms found in the oxygenated products of CO hydrogenation over $Rh_2O_3 \cdot 5H_2O$ do originate in CO and are not abstracted from the oxide lattice.

(1) The rate of production of oxygenates does not decrease with time.

(2) AES indicates that the working catalyst surface has a relatively low oxygen content. The total number of oxygen atoms found in the products generally exceeds that available in the sample.

(3) When the carbonaceous deposit, formed during a synthesis reaction, is hydrogenated in pure H_2, no trace of oxygen-

ated products is detected, yet hydrocarbons up to C_5 are produced. This evidence shows that in the absence of CO, oxygenated species do not form, while in the presence of CO they form in a manner indicating that CO incorporation is part of the reaction pathway. Thus it seems reasonable to propose that the aldehydic species formed during reaction arise from CO insertion into carbidic fragments present on the metal surface. The AES and rehydrogenation results with their similarity to those results seen for Fe (*17*) and Ni (*19*) indicate that a carbonaceous deposit is present on the surface of the working catalyst that contains little oxygen. Thus we would postulate that aldehyde formation occurs through CO insertion.

$$M\text{–}CH_x \xrightarrow{CO} M\text{–}CO\text{–}CH_x \xrightarrow{H} M + CH_3CHO, \quad (1)$$

$$M\text{–}C_2H_x \xrightarrow{CO} M\text{–}CO\text{–}C_2H_x \xrightarrow{H} M + CH_3CH_2CHO. \quad (2)$$

Support for this contention comes from two sources. First, we see almost complete carbonylation of C_2H_4 to C_2H_5CHO when ethylene is added to the reactant mixture. Second, rhodium is well known for its ability to catalyze the carbonylation of ethylene and methanol both in homogeneous (*18, 19*) and heterogeneous systems (*20, 22*). In these systems CO insertion into a $Rh\text{–}CH_3$ bond is thought to be the key step.

Important evidence to support this reaction mechanism is provided by our kinetic measurements. In particular, the activation energies for the formation of all hydrocarbons and acetaldehyde are all closely similar. This strongly suggests that these products all come from the same precursor with the same rate-determining step. The similarity of the activation energy for methane formation on both the oxide surface, rhodium metal, and the supported catalyst suggest that the mechanism for methane formation on all these surfaces is similar.

A way in which this data can be accommodated with a reaction mechanism is to postulate a rate-determining formation of surface metal–carbon species and then have efficient hydrogenation and carbonylation reaction steps. Once a $M\text{–}CH_x$ or similar species is formed, then it is rapidly and competitively converted to hydrocarbon or aldehyde.

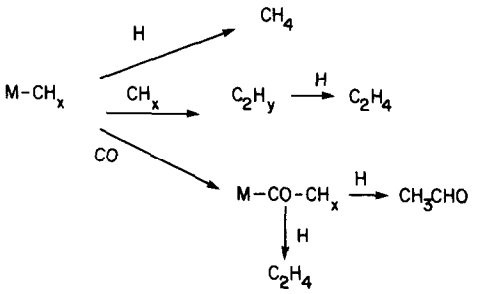

Chain growth could occur through addition of CH_x units, by CO insertion followed by hydrogenation or by condensation of two oxygenated intermediates. The data obtained through olefin addition suggest that when CO is inserted, the product aldehyde is released much more quickly than it can be hydrogenated, i.e., C_2H_5CHO is produced to the exclusion of C_3H_8. Hence, chain growth by insertion followed by hydrogenation to give hydrocarbon does not seem likely.

The actual product spectrum obtained will depend weakly on temperature as all activation energies are similar, and to a larger extent upon the H_2/CO ratio which will alter the balance between the competing secondary reactions.

While CO dissociation can occur on Rh surfaces under certain conditions (*27*), it has not been conclusively demonstrated to occur on rhodium oxide. Attempts to perform thermal desorption to investigate this possibility were hampered by a large background of CO produced by the reaction of carbon trapped in the bulk with lattice oxygen on heating. However, the TDS results do show that the bonding of both H_2 and CO on the active oxide surface differs markedly from those on the reduced metal surface. The relatively weaker bonding of

CO and stronger bonding of the H_2 to the oxide versus the metal surface correlates with the reduced hydrogenation capacity and increased tendency toward carbonylation of the oxide surface. However, it is difficult at this time to interpret these findings in mechanistic terms though it is hoped that further work in this area will clarify this question.

The spectroscopic results indicate that we are dealing with a partially reduced oxide possibly containing patches of metallic rhodium. It is interesting to note that rhodium in an oxidized form has been suggested as the active agent for carbonylation activity in a zeolite matrix (*24, 25*) as a result of ir, XPS, and uv measurements, although not conclusively (*26*). Also oxidized rhodium species are implicated as active centers in the homogeneous rhodium-catalyzed methanol carbonylation reaction (*18, 19*). It is possible that the oxide traps hydrogen as hydroxyls groups allowing carbonylation to compete successfully with hydrogenation and carbidic chain growth. Such ideas have been advanced by Sachtler and co-workers (*23*) as the formation of oxygenated products over iron Fischer–Tropsch catalysts occurring on oxide patches, possibly maintained by the water produced in the reaction.

CONCLUSIONS

1. While anhydrous RhO_2 and Rh_2O_3 are unstable to reduction under reaction conditions, $Rh_2O_3 \cdot 5H_2O$ is stable for long periods of time at temperatures <350°C.

2. This oxide is catalytically active for the hydrogenation of CO producing 25+ wt% of oxygenated products, mostly acetaldehyde, the balance being methane and C_2–C_5 alkenes.

3. The oxygenated products appear to form by insertion of CO into surface C_xH_y species; this process competes successfully on the oxide, but not on the reduced metal, with hydrogenation to hydrocarbons.

These results show that the reaction pathway that the hydrogenation of CO follows over rhodium surfaces can be drastically altered to produce oxygen-containing hydrocarbons instead of alkanes by placing the rhodium surface atoms into an oxide matrix. The ability to successfully produce oxygenated species by carbonylation appears to be linked to the higher than zero oxidation state of the rhodium. The hydrated $Rh_2O_3 \cdot 5H_2O$ catalyst undergoes partial reduction during pretreatment and eventual full reduction if used for a long enough period or at high enough temperatures. Work is under way to define and prepare more stable oxidized rhodium systems to further test the possibility of controlling the product distribution in the CO/H_2 reaction by the control of the oxidation state of the metal.

ACKNOWLEDGMENTS

This work was supported by the Director, Office of Energy Research, Office of Basic Energy Sciences, Chemical Sciences Division of the U. S. Department of Energy under Contract W-7405-ENG-48, and the Exxon Foundation. We thank Dr. R. Dodd (Lawrence Berkeley Laboratory) for taking the XPS data, and Drs. T. P. Wilson and J. A. Rabo for useful discussions.

REFERENCES

1. Vannice, M. A., *J. Catal.* **37**, 449 (1975).
2. Ichikawa, M., *Bull. Chem. Soc. Japan* **51**, 2268 (1978); *J. Catal.* **56**, 127 (1979).
3. Ellgen, P. C., Bartley, W. J., Bhasin, M. M., and Wilson, T. P., *ACS Advan. Chem. Ser.* **178**, 147 (1979).
4. Pruett, R. L., *Ann. N.Y. Acad. Sci.* **295**, 239 (1977).
5. Sexton, B. A., and Somorjai, G. A., *J. Catal.* **46**, 167 (1977).
6. Castner, D. G., Blackadar, R. L., and Somorjai, G. A., *J. Catal.* **66**, 257 (1980).
7. Blakely, D. W., Kozak, E. I., Sexton, B. A., and Somorjai, G. A., *J. Vac. Sci. Technol.* **13**, 1091 (1976).
8. Kim, K. S., and Winograd, N., *J. Catal.* **35**, 66 (1974).
9. Kim, K. S., and Winograd, N., *Surf. Sci.* **43**, 625 (1979).
10. Brinen, J. S., and Malera, A., *J. Phys. Chem.* **76**, 2525 (1972).
11. Jørgensen, C. K., and Berthou, G., *Det. K. Dan. Vidensk. Selsk. Mat. Fys. Medd.* **38**, 1 (1972).

12. Wentrec, P. R., Wood, B. J., and Wise, H., *J. Catal.* **43,** 363 (1976).
13. Araki, M., and Ponec, V., *J. Catal.* **44,** 439 (1976).
14. Goodman, D. W., Kelley, R. D., Madey, T. E., and Yates, J. T., Jr., *J. Catal.* **63,** 226 (1980).
15. Dwyer, D. J., and Somorjai, G. A., *J. Catal.* **52,** 291 (1978).
16. Krebs, H. J., and Bonzel, H. P., *Surf. Sci.* **99,** 570 (1980).
17. Bonzel, H. P., Krebs, H. J., and Schwarting, W., *Chem. Phys. Lett.* **72,** 165 (1980).
18. Paulik, F. E., and Roth, J. P., *Chem. Commun.*, 1578 (1968).
19. Hjortkjaer, J., and Jensen, V., *Ind Eng. Chem. Process Des. Dev.* **15,** 46 (1976).
20. Jarrell, M. S., and Gates, B., *J. Catal.* **40,** 255 (1975).
21. Yashima, T., Orikasa, Y., Takahashi, N., and Hara, N., *J. Catal.* **59,** 53 (1979).
22. Christensen, B., and Scurrell, M. S., *J. Chem. Soc. Faraday Trans. 1* **74,** 2313 (1978).
23. Biloen, P., Helle, J. N., and Sachtler, W. H. M., *J. Catal.* **58,** 95 (1979).
24. Primet, M., and Garbowski, E., *Chem. Phys. Lett.* **72,** 472 (1980).
25. Primet, M., Vedrine, J. C., and Naccache, C., *J. Mol. Catal.* **4,** 411 (1978).
26. Kuzniski, S., and Eyring, E. M., *J. Catal.* **65,** 227 (1980).
27. Castner, D. G., Dubois, L. H., Sexton, B. A., and Somorjai, G. A., *Surf. Sci.* **103,** L134 (1981).
28. Wunder, F., Arpe, H. J., Leupold, E. I., and Schmidt, H. J., U.S. Patent 4,224,236 (Hoescht AG).
29. Castner, D. G., and Somorjai, G. A., *Appl. Surf. Sci.* **6,** 29 (1980).
30. Muller, O., and Roy, R., *J. Less Common Metals* **16,** 129 (1968).
31. Yates, J. T., Thiel, P. A., and Weinberg, W. H., *Surf. Sci.* **84,** 427 (1979).
32. Castner, D. G., Sexton, B. A., and Somorjai, G. A., *Surf. Sci.* **71,** 519 (1978).